Available online at www.sciencedirect.com
ScienceDirect
Cement and Concrete Research 36 (2006) 1954–1968
Cement and Concrete Research

Inkbottle Pore-Method: Prediction of hygroscopic water content in hardened cement paste at variable climatic conditions

Rosa Maria Espinosa *, Lutz Franke

Lehr-und Forschungsbereich Bauphysik und Werkstoffe im Bauwesen, Hamburg University of Technology, Germany

Received 8 February 2005; accepted 28 June 2006

Abstract

The aim of this work is the development of a practicable method for the reliable prediction of the equilibrium hygroscopic water content in hardened cement paste and cement mortars at changing climatic conditions. Sorption thermodynamics and multi-scale pore structure of hardened cement paste build the basis of the new computation procedure. Drying and chemical aging lead to a formation of inkbottle pores. Their influence on sorption behaviour will be considered in particular by including them into the pore model. Experimental data of adsorption, desorption and scanning-isotherms verify the new computation method, which has been called "IBP-Method" (*i*nk*b*ottle *p*ores).

Keywords: Adsorption; Desorption; Hysteresis; Scanning-isotherms; Change of pore structure; Inkbottle pores

1. Introduction

The aim of this work is the development of a practicable method (called IBP-method) for the reliable prediction of the hygroscopic water content in hardened cement paste and cement mortars at changing climatic conditions.

In Ref. [8,10].the sorption behaviour of hardened cement paste was shown and discussed. These empiric data have provided the basis, which our *model for the structure* of cement gel has been deduced from. The developed IBP-method is based on this structure model and on sorption thermodynamics and it will be explained and discussed in this essay. It describes the hysteresis between adsorption and desorption isotherm and the (not trivial) paths between the sorption isotherms, frequently called "scanning-isotherms".

2. Measured sorption isotherms

The curing conditions were maintained constant at 100% r.h. and 23 °C. Thus material pores were continuously water-filled during curing. After 28 days the samples (5 mm·40 mm·40 mm) were stored at a constant temperature of 23 °C in decreasing relative humidity. The storage in the next stage of lower humidity took place after reaching weight equilibrium $m(\varphi)$.

Afterwards, the sample was dried to determine the reference weight m_0. The water content, which describes the first desorption (called basis-desorption), was calculated for each humidity with Eq. (1).

$$w(\varphi) = \frac{m(\varphi) - m_0}{m_0} \cdot 100 \tag{1}$$

Some measured sorption isotherms and scanning-isotherms were shown in a previous paper ([10]) and in Ref. [8,9]. Hereby the characteristics of the relevant sorption isotherms (basis-desorption, primary adsorption, secondary desorption and scanning-isotherms) were described. Two different drying methods (freezing-drying and standard-drying) were used and compared. Both, short-time and long-time measurements were performed.

3. Computation methods based on thermodynamics

There are several correlation methods (Künzel [16], Grunewald [14], T.C. Hansen [15] etc.) for the generation of sorption isotherms. The relevant parameters cannot be deduced physically, but have to be determined by adapting to empiric results. A further

* Corresponding author. Tel.: +49 40 42878 2056; fax: +49 40 42878 2905.
E-mail address: espinosa@tuhh.de (R.M. Espinosa).

0008-8846/$ - see front matter © 2006 Published by Elsevier Ltd.
doi:10.1016/j.cemconres.2006.06.011

disadvantage is that these equations are not applicable to the calculation of desorption isotherms and scanning-isotherms.

Therefore theoretically deduced models must be developed based on the theories of sorption and capillary condensation [5,12,13] and taking into account the properties of the pore structure of hardened cement paste and concrete [17–20,22–26]. In the following two theoretical models will be presented that can be used to calculate adsorption isotherms. The IBP method is based on these models, but offers the advantage of being able to predict the equilibrium water content at changing climate conditions.

3.1. Excess Surface Work method

Setzer and Adolphs [1–3] have developed a thermodynamic model called "Excess Surface Work" to calculate molecular (free) adsorption in non-porous and porous materials. The necessary parameters for this model do have a physical meaning.

The "Excess Surface Work" (shortened ESW) Φ is defined as follows:

$$\Phi := n_{\text{ads}} \cdot \Delta\mu \text{ or } \Phi = \Gamma \cdot A \cdot \Delta\mu < 0 \tag{2}$$

with n_{ads} the adsorbate amount in mol per g material, A the pore surface in m^2/g and $\Delta\mu$ the change of chemical potential during the adsorption in J/mol. At thermodynamical equilibrium between vapour molecules (d) and adsorbate (ads) results:

$$\Delta\mu = \Delta\mu_d = \Delta\mu_{\text{ads}} \text{ and } \Delta\mu_{\text{d}} = R \cdot T \cdot \ln \frac{p_{\text{d}}}{p_{\text{d,sat}}} \tag{3}$$

With p_{d} the vapour pressure and $p_{\text{d,sat}}$ the saturation vapour pressure.

The curve progression of ESW always exhibits a minimum, as Fig. 1 shows.

Adolphs defines the monolayer capacity n_{m} as the adsorbate amount at ESW minimum:

$$\frac{\partial \Phi}{\partial n_{\text{ads}}} = 0 \text{ at } n_{\text{ads}} = n_{\text{m}} \tag{4}$$

The monolayer capacity n_{m} represents the adsorbate amount to cover the solid surface (i.e. pore wall) with only one layer of water molecules. If the adsorbate becomes thicker, the interaction force between surface and adsorbate decreases and therefore so does the surface energy during adsorption. For this reason ESW tends to zero.

The relation between the chemical potential and adsorbate amount must satisfy Eqs. (3) and (4). Adolphs and Setzer deduced the following linear relation considering numerous experimental results:

$$n_{\text{ads}} = -n_{\text{m}} \cdot \ln \left| \frac{\Delta\mu}{\Delta\mu_0} \right| \tag{5}$$

$\Delta\mu_0$ is the chemical potential to adsorb the first molecule ($n_{\text{ads}} \to 1$), i.e. the start-potential. Since the start potential is negative, the adsorption begins at a vapour pressure above null ($p_{\text{d}} > 0$ or $\varphi > 0$).

The necessary material parameters n_{m} and $\Delta\mu_0$ for this model must be acquired by fitting Eq. (5) to adsorption data.

The specific pore surface A (in m^2/g) is given by:

$$A = n_{\text{m}} \cdot A_{\text{mol}} \cdot N_A \tag{6}$$

with A_{mol} the surface of an adsorbed molecule (for water about 10.6 A^2) and N_{A} the Avogadro's number ($6.022 \cdot 10^{23}$). Thus the pore surface does not describe the real geometrical pore surface, since it also depends on the interaction forces between adsorbate and material.

Usually water content (w) is given in M. — % instead of in mol/g. The following equation gives the relation between them:

$$w = n_{\text{ads}} \cdot M \cdot 100 \text{ or } w = -\frac{A \cdot M}{A_{\text{mol}} \cdot N_{\text{A}}} \cdot \ln \left| \frac{\Delta\mu}{\Delta\mu_0} \right| \cdot 100 \tag{7}$$

with M the mol mass of water.

The measured adsorption isotherms of porous materials fit very well with Eq. (5), if no capillary condensation takes place. According to Adolphs's experimental results [3] the relation between adsorbate and chemical potential in case of capillary condensation satisfy a similar equation:

$$n_{\text{cond}} = -n_m \cdot \theta \cdot \ln \left| \frac{\Delta\mu}{\Delta\mu_1} \right| \tag{8}$$

with $\Delta\mu_1$ the chemical potential and θ the number of existing adsorbate layers on the pore wall, both at the beginning of capillary condensation. The calculation of capillary condensate needs two more material parameters: $\Delta\mu_1$ and θ.

Adolphs calls his method to calculate adsorption and capillary condensation in porous materials "Excess Surface Work" with 4 parameters. Contrary to most correlation methods these parameters have a physical meaning. They depend on the pore structure and on the interaction force between hardened cement paste matrix and water. If the four material parameters are known, the adsorption isotherm can be computed.

In principle it is also possible to calculate desorption isotherms. However further four material parameters are necessary, which makes the disadvantage of this method evident: A great number of parameters have to be analysed first by fitting experimental results. Furthermore the scanning-isotherms cannot be predicted by means of ESW.

3.2. Excess Surface Work and Disjoining Pressure Isotherm method (ESW-DPI)

The Excess Surface Work method is also used for the description of molecular adsorption. However Eq. (5) is rewritten as a function of the disjoining pressure Π. Thus this equation is called "disjoining pressure isotherm" [6] of an even adsorbate film:

$$\Pi = \Pi_0 \cdot \exp\left(\frac{-h}{h_{\text{m}}}\right) \tag{9}$$

with $\Delta\mu = v_{\text{m}} \cdot \Pi$ the chemical potential, h the thickness of the adsorbate layer, h_{m} the thickness of a monolayer adsorbate film

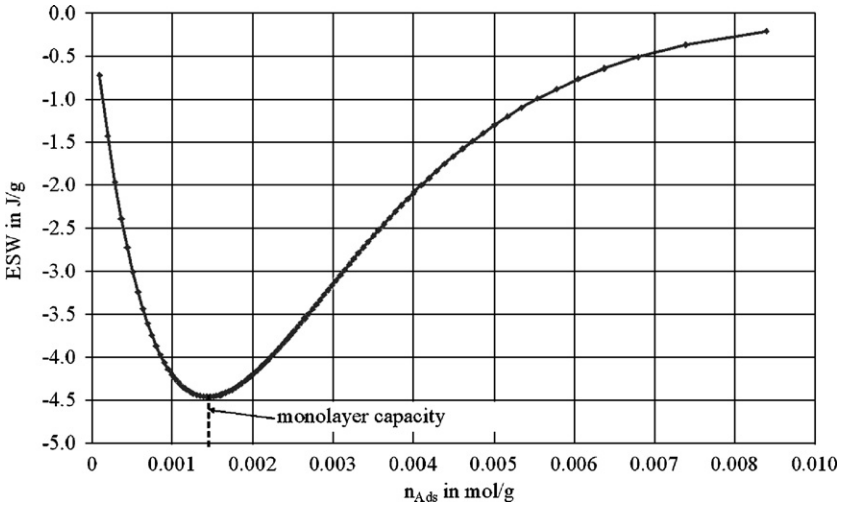

Fig. 1. Typical form of ESW and monolayer capacity.

(for water 2.8 A) and $v_m = 18 \cdot 10^{-6}$ mol/m^3 the adsorbate mol volume [13]. The parameter Π_0 characterizes the surface forces between an even film and the solid.

The use of disjoining pressure is based on the theory of thin films (by Derjaguin [7], Bazant [4]). If a very thin film (<2 nm) fills the gap between two solid surfaces (e.g. a micro pore), the interaction due to repulsion, electrostatic and van der Waals forces is significantly higher than in meso or macro pores. Indeed an average pressure tries to disjoin the solid surfaces. Actually, the disjoining pressure leads to stability of CSH-Phases.

Assuming that $\ln(\Delta\mu_0) = 9.08$ for Portland hardened cement paste it follows that $\Pi_0 = -\Delta\mu_0 / v_m = 488$ MPa. Thus the disjoining pressure for $h = 0.5$ nm is equal to 82 MPa. This pressure acts on the pore wall (micro structure), so it cannot be assumed to be macroscopic pressure (this is significantly smaller).

Disjoining pressure decreases exponentially with increasing gap size. Thus it is equal to 2.3 MPa for $h = 1.5$ nm, while the capillary pressure acting in these pores is equal to 115 MPa. Thus disjoining pressure can be neglected in meso gel pores.

The pore size distribution and the assumption of a pore geometry are necessary for the computation of capillary condensation and desorption according to the ESW-DPI method instead of $\Delta\mu_1$ and θ (see Section 3.1).

The thermodynamical equilibrium between curved adsorbate film (water film) and vapour, satisfy the next equation in cylindrical pores (radius r):

$$\varnothing(h) = \Pi_0 \cdot \exp\left(\frac{-h}{h_m}\right) + \frac{\sigma}{r-h} = -\frac{R \cdot T}{v_m} \cdot \ln\varphi_{\text{cap.cond.}} \qquad (10)$$

Since the interface between vapour and water film covering cylindrical pore walls is curved, the surface tension σ (N/m) acts on the film (contact angle = 0°). $\varnothing(h)$ gives the average pressure which acts on a curved adsorbate under the action of the disjoining pressure.

According to Derjaguin the stability condition of thin films is given by a minimization of $\varnothing(h)$. At the minimum of $\varnothing(h)$ the film becomes unstable and collapses, filling the pore completely. Thus capillary condensation takes place.

The minimization of $\varnothing(h)$ leads to the following relation between pore radius (r^*) and thickness of the adsorbate layer (h^*) at capillary condensation in each pore:

$$\frac{1}{h_m} \cdot \Pi_0 \cdot \exp\left(\frac{-h^*}{h_m}\right) = \frac{\sigma}{(r^* - h^*)^2} \qquad (11)$$

The next equation gives the disjoining pressure isotherm for capillary desorption in cylindrical pores:

$$\frac{2\sigma}{r-h} = -\frac{R \cdot T}{v_m} \ln\varphi_{\text{cap.des.}} \qquad (12)$$

with $h = -h_m \cdot \ln\left|\frac{\Pi}{\Pi_0}\right|$.

The given (Eqs. (10)–(12)) render the functional relation between pore radius and relative humidity for capillary condensation and capillary desorption. These functions are shown in Fig. 2 (for capillary condensation and for capillary desorption). They were computed for a value $\ln(-\Delta\mu_0) = 9{,}04$.

For other pore geometries (e.g. slit pores, spherical pores) similar equations can be deduced.

4. Model for the structure of hardened cement paste

The structure model for hardened cement paste was described in detail in Ref. [10]. The following reasons for the hysteresis between adsorption and desorption were deduced:

- Existence of a different curvature of the interface liquid–vapour before capillary condensation and capillary desorption as a function of pore geometry. The relative humidity for capillary condensation and desorption in cylindrical and inkbottle pores will be deduced in Sections 5.1 and 5.6.1.
- Drying and chemical aging cause a compression of cement gel particles. Hence some gel pores become enclosed by the compressed cement gel. They are only accessible through very small pore radii (smaller than 1 nm), so that they behave as inkbottle pores. Additionally the capillary pore volume increases due to the compression.

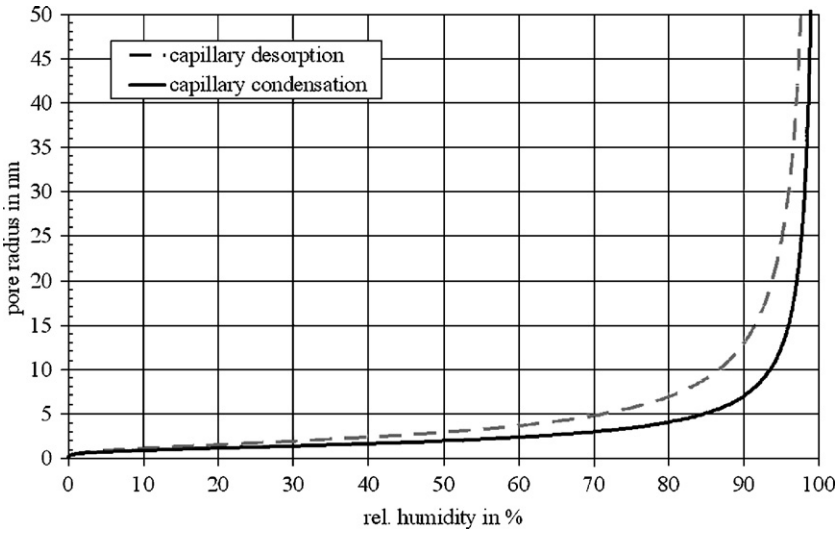

Fig. 2. Relation between pore size and humidity for capillary condensation and capillary desorption under assumption of cylindrical pores.

— The continuation of cement hydration during sorption measurements (i.e. during storage at changing climatic conditions) causes a change of porosity (more gel pores and fewer capillary pores) and an increase of the dry weight. Both of them affect the hygroscopic humidity content. The influence of the hydration degree on the hygroscopic humidity content can be calculated by the ratio of hydrated hardened cement paste.

5. IBP method to predict basis-desorption and primary adsorption

Basis-desorption and primary adsorption must be known, if the hygroscopic water content at changing climatic conditions (scanning-isotherms) is to be determined using the IBP method. Basis-desorption and primary adsorption can be measured and/or taken out of literature data, respectively. An alternative method for the estimation of Basis-desorption and primary adsorption is described in this section. It is based on sorption thermodynamics and on the developed structure model for hardened cement paste.

The basis for the new method is the ESW-DPI procedure, which was described in Section 3.2. The pore size distribution of the material is required for the calculation. We chose the mercury pressure porosimetry to describe it, since this method is often used worldwide.

Actually, it is well-known that the mercury pressure porosimetry does not describe the real pore structure. Generally, the amount of smaller pores is overestimated. The material parameters for the IBP-method (form factors *f*, see p. 26) include the influence of the measurement method for the pore size distribution. If other technique is used, new values for the form factors have to be obtained.

At first only cylindrical pores will be used. Later the influence of existing inkbottle pores on desorption and sorption will be introduced by adapting the measured pore size distribution.

A pore model is a rough simplification of the real pore structure. Actually, it has to be considered as a complicated network of different pore forms and connections. According to recent investigations about the structure and form of CSH phases [21] the gel pores can surely be modelled better as slit pores. Slit pores with closed ends lead to a complicated mathematical description of the problem, which requires several simplifications to solve it. Since the assumption of cylindrical and inkbottle pores is in good agreement with experimental results, a modelling of slit pores will be abandoned.

5.1. Desorption and sorption theory in cylindrical pores

The classical model assumes that a cylindrical interface adsorbate-vapour builds up in cylindrical pores with two open sides, before capillary condensation begins. Before capillary desorption starts, a hemispherical interface is present at both pore ends. The interaction force between solid and adsorbate will be neglected in meso gel pores according to Section 3.1. In Ref. [10] (see Fig. 10) the menisci for capillary condensation and desorption in cylindrical pores are depicted. The following equations for the relative humidity were deduced:

$$\varphi_{\text{cap.cond.}} = \exp\left(-\frac{\sigma \cdot v_{\text{L}}}{R \cdot T \cdot (r^{\text{P}} - h)}\right)$$
$$\varphi_{\text{cap.des.}} = \exp\left(-\frac{2 \cdot \sigma \cdot v_{\text{L}}}{R \cdot T \cdot (r^{\text{P}} - h)}\right) \tag{13}$$

Considering that the thickness of the adsorbate layer is a function of the relative humidity, both equations are related as it follows:

$$\frac{r^{\text{P}} - h(\varphi_{\text{cap.des.}})}{r^{\text{P}} - h(\varphi_{\text{cap.cond.}})} \cdot \ln\varphi_{\text{cap.des.}} = 2 \cdot \ln\varphi_{\text{cap.cond.}} \tag{14}$$

If the influence of the different humidity on the thickness of the adsorbate layer (in Eq. (14)) is neglected, h can be simplified. This leads to the following relation between rel. humidity for capillary condensation and for capillary desorption:

$$\ln\varphi_{\text{cap.des.}} = 2 \cdot \ln\varphi_{\text{cap.cond.}} \Rightarrow \varphi_{\text{cap.des.}} = \varphi^2_{\text{cap.cond.}} \tag{15}$$

Thus the condensate, which was taken up to $\varphi_{cap.cond.}$, will be extracted from the pores at ${\varphi^2}_{cap.cond.}$. The resulting hysteresis between capillary condensation and capillary desorption in cylindrical pores was shown in Fig. 11 in Ref. [10].

If one pore side is closed, a hemispherical meniscus forms before capillary condensation as well as before capillary desorption. The radius of curvature results $r_m = r^P - h$ for both mechanisms. In this case it yields no hysteresis.

5.2. Basis-desorption isotherm considering cylindrical pores

Eq. (12) gives $\varphi_{cap.des}$ for capillary desorption. The following constants will be assumed:

Mol volume v_m	$18 \cdot 10^{-6}$ m^3/mol
Thickness of monolayer of water molecules h_m	2.8 A
Surface tension of water σ	0.0723 N/m
Gas constant R	8.314 J/(mol K)
Temperature	296.13 K

Substituting the constants in Eq. (12) it yields the following function to calculate $\varphi_{cap.des}$:

$$\varphi_{cap.des} = \exp\left(-\frac{18 \cdot 10^{-6}}{2460} \cdot \frac{0.1446}{r-h}\right) \quad (16)$$

The function $\varphi_{cap.des}$ depends on pore radius (r) and thickness of adsorbate layer (h). Therefore an additional equation is necessary to relate h with the pore radius or with the relative humidity.

According to the ESW-DPI method the function $h(r)$ during capillary condensation is given by Eq. (11). This equation, however, leads to a bad fitting to our experimental results. Thus it will not be used in our own computation method. A much better assimilation results from the following empirical equation:

$$h = 0.395 - 0.189 \cdot \ln(-\ln\varphi) \text{ in nm (in Ref. [23])} \quad (17)$$

The solution of the system of equations consisting of Eqs. (16) and (17) is iterative. The result is a function for the desorption isotherm depending only on the pore radius $\varphi_{cap.des}(r)$.

The water content for the Basis-desorption $w_D(\varphi_{cap.des})$ will be calculated as follows:

$$w_D(\varphi_{cap.des}) = w_h(\varphi_{cap.des}, r \geq R) + w_p(r<R) \text{ with } \varphi_{cap.des}(R) \text{ according to Eq. 16} \quad (18)$$

with R the radius of the pores, in which capillary desorption takes places. The following terms must be determined:

- $w_h(\varphi_{cap.des},\ r \geq R)$ is the adsorbate amount filling the pores which are already free of capillary condensate.
- $w_P(r<R)$ the water content (adsorbate and capillary condensate) filling the pores in which capillary desorption has not yet started (they are too small).

The determination of these terms will be described in Section 5.4.

5.3. Primary adsorption isotherm considering cylindrical pores

The same constants as in Section 5.2 will be used to calculate the relative humidity for capillary condensation using Eq. (10) at 23 °C:

$$\varphi_{cap.cond} = \exp\left(\frac{\Delta\mu_0}{2460} \cdot \exp\left(\frac{-h}{2,8 \cdot 10^{-10}}\right) - \frac{18 \cdot 10^{-6}}{2460} \cdot \frac{0,0723}{r-h}\right) \quad (19)$$

$\varphi_{cap.cond.}$ depends on pore radius and thickness of the adsorbate layer. Therefore Eq. (18) is also required.

In this case the method to solve the system of equations consisting of Eqs. (17) and (19) is iterative again. The result is a function for the relative humidity dependent only on the pore radius: $\varphi_{cap.cond.}(r)$.

The *primary adsorption* results:

$$w_A(\varphi_{cap.cond}) = w_h(\varphi_{cap.cond}, r>R) + w_P(r \leq R) \textit{ mit } \varphi_{cap.cond}(R) \text{ according to Eq. 19} \quad (20)$$

with R the radius of the pores, in which capillary condensation takes place. The following terms must be determined:

- $w_h(\varphi_{cap.cond.},\ r>R)$ is the adsorbate amount that fills the pores which are still free of capillary condensate.
- $w_P(r \leq R)$ the water content (adsorbate and capillary condensate) filling the pores in which capillary condensation has already taken place.

The determination of these terms will be described in the next section.

5.4. Water content as a function of pore radius (w_h and w_P)

The pore size distribution measured by means of mercury pressure porosimetry gives the pore volume V_P corresponding to each pore radius. The cumulative pore size distribution $V_P(r)$ (in ml/g) can be converted into water content $w_P(r)$ using the water density and the saturation content w_{sat}:

$$w_P(r) = w_{sat} - V_P(r) \cdot \rho_w \cdot 100 \text{ in } M.-\%, \text{with } \rho_w = 1 \text{ g/cm}^3 \quad (21)$$

If the cumulative pore size distribution is represented with decreasing pore radius along the x-axis. The calculated (cumulative) water content $w_P(r)$ consists of adsorbate and capillary condensate amount (Fig. 3).

The mercury pressure porosimetry cannot measure gel pores smaller than 1.8 nm. These pores include a pore volume equal to approximately 10 vol.%. Hence the computed water content w_P does not start with zero at the smallest measured pore radius (r_{min}).

The Basis-desorption begins at pore saturation $w_{sat} = w_P$ (r_{max}), as all pores are water-filled. The calculation starts at the

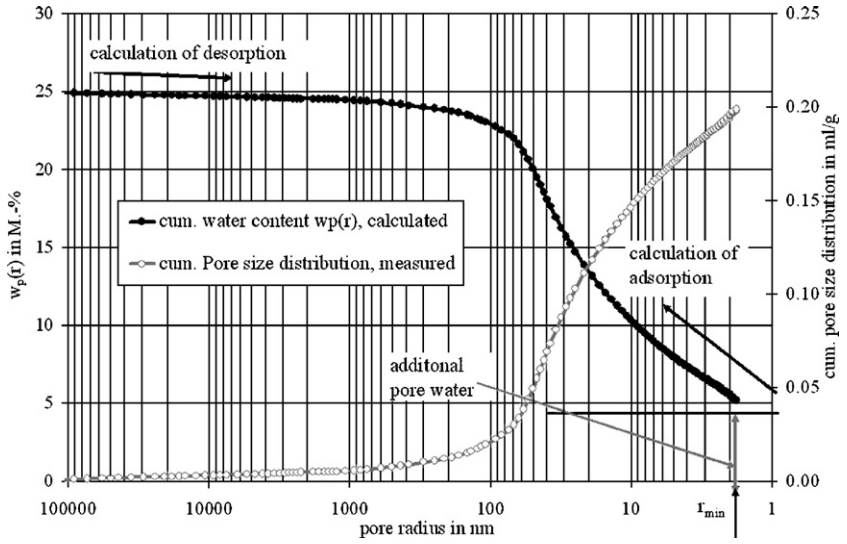

Fig. 3. Transformation of the cumulative pore size distribution (in ml/g) into water content (in M.-%). Material: ZAB 12Mon w/c 0.50.

largest pore radius and reproduces the drying process of the pores from the highest (r_{max}) to the smallest (r_{min}) measured pore radius.

In contrast the calculation of the primary adsorption starts at r_{min}. In this state all pores with a radius smaller than r_{min} are filled with water. It continues filling the pores from minimal to maximal measured pore radius and ends at saturation.

The calculated water content $w_P(r)$ gives both adsorbate and capillary condensate in the pores with radius $r \le R$. However an additional term must be regarded, i.e. w_h in equations Eqs. (18) and (20).

During basis-desorption a quantity of adsorbate remains in the pores ($r \ge R$), where capillary desorption already took place. This quantity is given by the following equation:

$$w_h(\varphi_{Kap.Des}) = h(\varphi_{Kap.Des}) \cdot A(r \ge R) \cdot \rho_w \cdot 100 \text{ in } r \ge R \qquad (22)$$

The thickness of the adsorbate layer depends on the humidity according to Eq. (17). $A(r \ge R)$ is the specific surface of pores free of capillary condensate and ρ_w is the water density. The mercury pressure porosimetry supplies the pore surface as a function of the pore radius.

In case of a primary adsorption an additional quantity of adsorbate is present in the pores, in which capillary condensation has not yet begun due to their large size ($r > R$). This quantity w_h is computed as follows:

$$w_h(\varphi_{Kap.Kond}) = h(\varphi_{Kap.Kond}) \cdot A(r > R) \cdot \rho_w \cdot 100 \text{ in } r > R \qquad (23)$$

$h(\varphi)$ will be calculated according to Eq. (17).

Thus the water content as function of the pore radius is known. Furthermore the function which converts the pore radius r in the associated relative humidity for capillary condensation and for capillary desorption was deduced for cylindrical pores in Sections 5.2 and 5.3.

The water content in the non-measured pores ($r < 1.8$ nm) is calculated by means of the ESW equation (Eq. (7)):

$$\begin{aligned} w &= -\frac{A \cdot M}{A_{mol} \cdot N_A} \cdot \ln\left|\frac{\Delta\mu}{\Delta\mu_0}\right| \cdot 100 \\ &= -0.0282.A \cdot \ln\left|\frac{\Delta\mu}{\Delta\mu_0}\right| \text{ in } M.-\% \text{ with } \Delta\mu \\ &= R \cdot T \cdot \ln(\varphi) \text{ in J/mol} \end{aligned} \qquad (24)$$

with M the mol mass of water (18 g/mol), A_{mol} the surface of an adsorbed water molecule (10.8 A^2) and N_A the Avogadro's number ($6.023 \cdot 10^{23}$).

The following input data are necessary for the calculation of the Basis-desorption and the primary adsorption:

- Start potential for the adsorption $\Delta\mu_0$ and specific pore surface A.
- Saturation content w_{sat} determined by water uptake under pressure and drying.
- Cumulative pore size distribution and the assumption of a pore model.

The pore surface and the start potential can be acquired by means of the ESW Method (see Section 5.5).

The cumulative pore size distribution is measured assuming a cylindrical pore model. Furthermore inkbottle pores build up during drying and chemical aging according to the developed structure model. Inkbottle pores have a significant influence on adsorption and desorption. Hence the introduction of a new pore model consisting of inkbottle pores is necessary. The modelling of inkbottle pores will be described in Section 5.6.

5.5. Use of the ESW method to estimate the start potential and the specific pore surface

The ESW equation gives a linear relation between the adsorbate quantity and the logarithm of the chemical potential (see Eq. (5)).

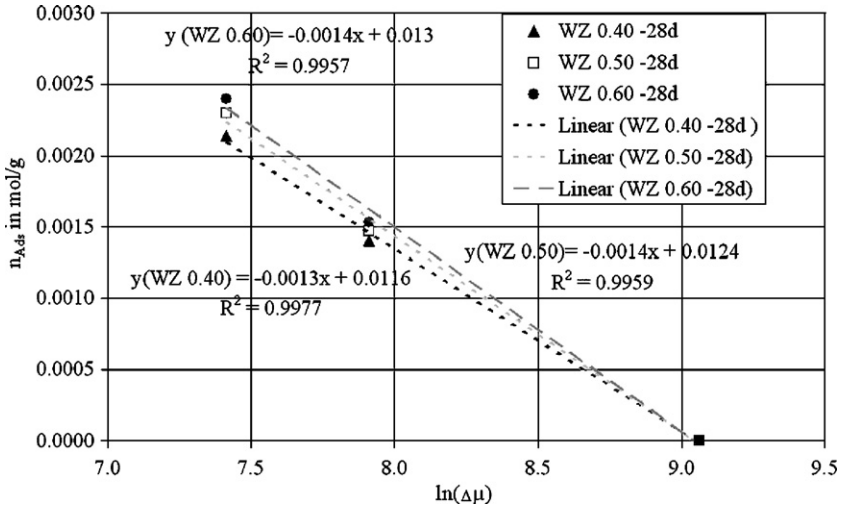

Fig. 4. Water content (in mol/g) as function of chemical potential (data of primary adsorption between 3 and 50% r.h.).

Let us have a look at the measured adsorption isotherm of hardened cement paste at the age of 28 days. Fig. 4 shows the measured water content (in mol/g) in relation to the respective chemical potential.

The measured data fit very well to a linear regression,

$$n_w = a \cdot \ln(|\Delta\mu|) + b \text{ or } \Delta\mu = -\exp\left(\frac{n_w - b}{a}\right) \tag{25}$$

Furthermore the relation between adsorbate amount and chemical potential must fulfil the condition of the energetic minimum according to Eq. (4). It follows that the parameter a is equal to the monolayer capacity n_m:

$$\frac{\partial \Phi}{\partial n_w} = \frac{\partial(n_w \cdot \Delta\mu)}{\partial n_w} = \frac{\partial\left(n_w \cdot \left(-\exp\left(\frac{n_w - b}{a}\right)\right)\right)}{\partial n_w} = 0$$

$$\frac{\partial \Phi}{\partial n_w} = -\exp\left(\frac{n_w - b}{a}\right) - n_w \cdot \exp\left(\frac{n_w - b}{a}\right) \cdot \frac{1}{a} = 0$$

$$\text{Minimum at } n_w = n_m \Rightarrow 0 = 1 + n_m \cdot \frac{1}{a} \Rightarrow -a = n_m \tag{26}$$

At the beginning of the adsorption (n_w=0, Φ=0) the chemical potential is negative and equal to the start potential $\Delta\mu_0$. This can be calculated with parameters a and b:

$$\Delta\mu|_{n=0} = -\exp\left(\frac{0 - b}{a}\right) = \Delta\mu_0 \text{ (start potential)} \tag{27}$$

For the linear regression the parameters a (slope) and b (intersection with y-axis) can be determined graphically. For ZAB 28d w/c 0.60 a=−0.0014 and b=0.013. It follows that n_m=0.0014 mol/g and ln($\Delta\mu_0$)=9.06.

The specific pore surface (with A_{mol}=10.8 A^2 and N_A=$6.022 \cdot 10^{23}$) amounts to 91.1 m^2/g. Further values are given in Table 1.

The slope of the Excess Surface Work at n_w=0 is equal to the start potential. The negative start potential leads to a positive relative humidity. That means, a positive relative humidity is necessary for starting adsorption:

$$\begin{aligned}\Delta\mu_0 &= R \cdot T \cdot \ln(\varphi_0) \Rightarrow \varphi_0 \\ &= \exp\left(\frac{\Delta\mu_0}{R \cdot T}\right) > 0 \text{ for } \ln(-\Delta\mu_0) = 9.06,\ T \\ &= 296.15 \text{ K} \Rightarrow \varphi_0 = 3.0\%\end{aligned} \tag{28}$$

5.6. Modelling inkbottle pores

According to the developed structure model [9,10] inkbottle pores build up in the pore system of hardened cement paste. Thus they significantly influence the sorption behaviour and the hysteresis between desorption and adsorption. This will be deduced in Section 5.6.1.

The goal of this section is to introduce inkbottle pores into the pore size distribution, which was measured by means of mercury pressure porosimetry considering only cylindrical pores. The new pore size distribution $V_P(r_{neu})$ is used to calculate Basis-desorption and primary adsorption using the equations explained in Section 5.1.

5.6.1. Desorption and sorption in inkbottle pores

According to the classical model, inkbottle pores consist of two cylindrical pores with different radii (Fig. 5).

Table 1
Approximation parameters for Portland hardened cement paste (ZAB), determined by fitting measured primary adsorption isotherms according to ESW. Drying method: Standard drying. The decrease of the pore surface with increasing age is due to chemical aging

Material	log ($\Delta\mu_0$)			A in m^2/g		
ZAB	w/c 0.40	w/c 0.50	w/c.60	w/c 0.40	w/c 0.50	w/c 0.60
28d	9.05	9.04	9.04	82.0	88.1	91.1
12Mon	9.05	9.02	9.08	76.5	102.1	104.9
26Mon	9.05	9.06	9.07	73.8	82.6	87.4
Mean value	9.1 (0.2%)			87.7 (12%)		

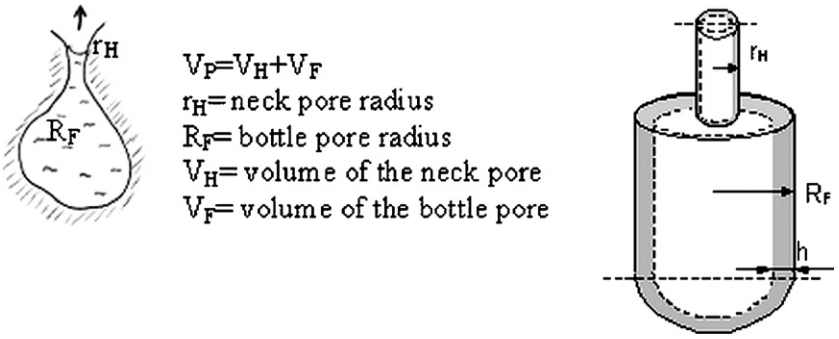

Fig. 5. Classical modelling of inkbottle pores.

The "neck" (smaller radius r_H) is connected with a "bottle" (larger radius R_F), the closed bottom of which exhibits a hemispherical form.

Before capillary condensation sets, the adsorbate film exhibits a cylindrical surface on neck and bottle pore wall, while a hemispherical meniscus is present at the bottom of the bottle pore. This leads to different air humidities for the filling of neck and bottle pore by means of the Kelvin-equation ($r>1$ nm):

$$\text{neck pore} \Rightarrow r_m = 2\cdot(r_H - h) \Rightarrow \varphi_{cap.cond,H} = \exp\left(-\frac{\sigma\cdot v_m}{R\cdot T\cdot(r_H - h(\varphi_{cap.cond,H}))}\right)$$

$$\text{bottle pore} \Rightarrow r_m = (R_F - h) \Rightarrow \varphi_{cap.cond,F} = \exp\left(-\frac{2\cdot\sigma\cdot v_m}{R\cdot T\cdot(R_F - h(\varphi_{cap.cond,F}))}\right) \quad (29)$$

It has to be remarked, that the interaction force Π in meso pores was not regarded.

Depending on the relation R_F to r_H two different filling mechanisms of the inkbottle pore can take place during capillary condensation:

— if $(R_f - h(\varphi_{Kap.Kond,F})) > 2\cdot(r_H - h(\varphi_{Kap\cdot Kond,H}))$, $\varphi_{Kap\cdot Kond,F} > \varphi_{Kap\cdot Kond,H}$, i.e. the neck ($V_H$) fills first at $\varphi_{Kap\cdot Kond,F}$ and at $\varphi_{Kap\cdot Kond,F}$ the bottle pore (V_F) fills.

— if $(R_f - h(\varphi_{Kap.Kond,F})) < 2\cdot(r_H - h(\varphi_{Kap\cdot Kond,H}))$, bottle and neck pore ($V_H + V_F$) fill at $\varphi_{Kap\cdot Kond,F}$. Capillary condensation begins at the bottom of the bottle pore and continues, until the neck pore is also filled at constant humidity.

Before emptying the total pore volume ($V_H + V_F$) a hemispherical meniscus is present at the neck opening. The radius of curvature is $r_m = r_H - h$. The corresponding humidity for capillary desorption results:

$$\varphi_{cap.des} = \exp\left(-\frac{2\cdot\sigma\cdot v_m}{R\cdot T\cdot(r_H - h(\varphi_{cap.des}))}\right) \quad (30)$$

By reaching this humidity the water will be excluded from the whole inkbottle pore.

A material parameter (f) for the characterisation of inkbottle pores will be introduced. This gives the relation between R_F and r_H ($f = R_F/r_H$).

If $\frac{R_F - h(\varphi_{cap.cond,F})}{r_H - h(\varphi_{cap.cond,H})} > 2$, the relation between humidity for capillary condensation and capillary desorption for the neck pore results:

$$\ln\varphi_{cap.des.} = 2\cdot\frac{r_H - h(\varphi_{cap.cond,H})}{r_H - h(\varphi_{cap.des})}\cdot\ln\varphi_{cap.cond,H} \quad (31)$$

and for the bottle pore:

$$\ln\varphi_{cap.des.} = \frac{f\cdot r_H - h(\varphi_{cap.cond,F})}{r_H - h(\varphi_{cap.des})}\cdot\ln\varphi_{cap.cond,F} \quad (32)$$

If $\frac{R_F - h(\varphi_{cap.cond,F})}{r_H - h(\varphi_{cap.cond,H})} \le 2$, then Eq. (33) gives the relation between relative humidity for capillary condensation and for capillary desorption of the total pore volume $V_H + V_F$:

$$\ln\varphi_{cap.des.} = \frac{f\cdot r_H - h(\varphi_{cap.cond})}{r_H - h(\varphi_{cap.des})}\cdot\ln\varphi_{cap.cond.} \quad (33)$$

In the last case capillary desorption is determined by the radius of curvature of the hemispherical meniscus at the neck pore opening, while capillary condensation is determined by the curvature radius of the hemispherical meniscus at the bottom of the bottle pore.

5.6.2. Introduction of inkbottle pores into the pore size distribution

The bottle pore (with radius R_F) cannot empty at a humidity $\varphi_{cap.des}(R_F)$, but only at a smaller humidity according to the neck pore $\varphi_{cap.des}(r_H) < \varphi_{cap.des}(R_F)$. This leads to a pronounced hysteresis between the adsorption and the desorption isotherm.

The real pore system will be modelled as a network of inkbottle pores.

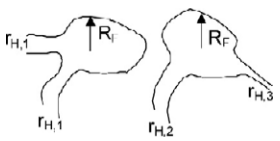

A bottle pore can be connected with several neck pores. Besides there are several bottle pores with the same pore radius R_F, which are connected with different neck pores.

In the following two methods for the mathematical modelling of inkbottle pores will be described.

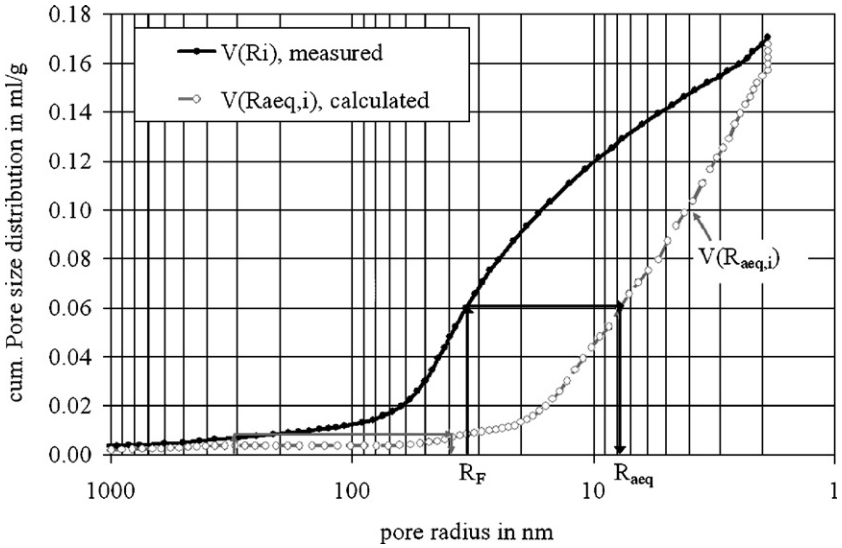

Fig. 6. Cumulative pore size distribution of ZAB-2 28d w/c 0.40: measured pore radii R_i and computed equivalent neck pore radii $R_{aeq,i}$.

5.6.2.1. Modelling of inkbottle pores using equivalent neck pore radii. The mercury pressure porosimetry gives the total pore volume to each size. A distinction between pore volumes of the bottle pores, which are connected with different neck pores, cannot be accomplished.

In order to consider different neck-bottle connections, an equivalent neck pore radius $R_{aeq,i}$ will be computed for each measured pore (R_i) as follows:

$$\text{For each } R_i \Rightarrow R_{aeq,i} = \frac{\sum_i r_i}{n_{r_i}} \forall\ r_i < R_i \tag{34}$$

r_i is the radius of all measured pores smaller than R_i and n_{ri} is the number of pores with radius r_i. In the standard case it will be assumed that all measured pores with radius $r_i < R_i$ can be regarded as neck pores of the bottle pore (R_i).

The curve in Fig. 6 gives the cumulative pore size distribution $V(R_{aeq,i})$. The equivalent neck pore radii $R_{aeq,i}$ were calculated with Eq. (34) for each measured pore (R_i).

As an example, for those pores with a radius equal to 32 nm capillary desorption does not set in until the relative humidity is reached which results for the equivalent radius of 7.2 nm. Similarly capillary desorption sets in pores with radius equal to 300 nm at the relative humidity according to the equivalent radius of 35 nm.

5.6.2.2. Modelling of inkbottle pores using a form factor. The smaller the neck pore radius becomes, the more significant is the effect of inkbottle pores on the desorption, since the humidity for the capillary desorption decreases more strongly.

For the characterisation of inkbottle pores a form factor was introduced in Section 5.5. This gives the relationship of the measured pore radius R_i (a cylinder) to the neck pore radius $r_{H,i}$.

$$f_i^* = \frac{R_i}{r_{H,i}} \tag{35}$$

It is necessary to consider two kinds of inkbottle pores by means of using two different form factors:

— Drying of capillary water will be modelled by inkbottle pores with form factor f^*_{Kap}. The complete drying of capillary pore water is only possible if water transport takes place through small gel pores. This can be described by inkbottle pores, whose neck pores are the gel pores and whose bottle pores are the capillary pores. Our own investigations show that the drying of capillary pore water has to be considered above 70–80% r.h. Below 70% r.h. there is no more capillary pore water in the pore system (or only a few). This means that the smallest effective neck pore radius for capillary water has a range of 5–7 nm.

— Intensive drying processes and chemical aging also lead to the formation of inkbottle pores in cement gel due to its compression. The cumulative pore size distribution shows that the portion of gel pores ($r < 10$ nm) has decreased after drying and chemical aging. Smaller neck pores prevent the intrusion of mercury into these pores.

f^* is considered as constant in the two pore size ranges to simplify the model.

Thus the pore size distribution of the neck pores is calculated with a factor f^*_{Kap} and/or f^*_{Gel}. The border radius for the application of the two form factors lies between 5 and 10 nm. For the following computations the border radius is set equal to 5 nm:

$$r_{H,i} = \frac{R_i}{f^*},\ \text{with } f^* = f^*_{Kap} \text{ for } R_i > 5 \text{ nm and with } f^* = f^*_{Gel} \text{ for } R_i < 5 \text{ nm} \tag{36}$$

The assumption of a boundary radius of 10 nm also leads to a good compliance with the empiric results. In this case smaller form factors are needed (about 25% smaller).

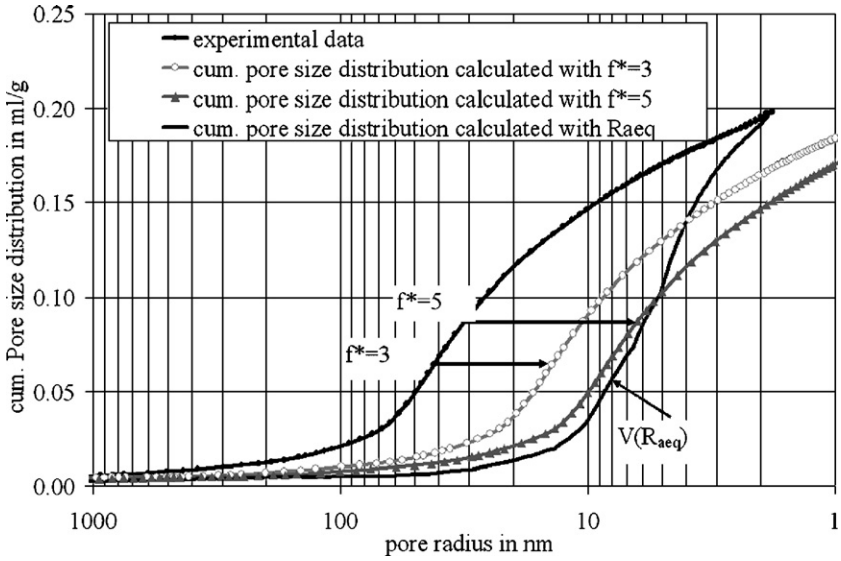

Fig. 7. Computed pore size distribution considering equivalent neck pore radii and using different form factors f^*. Material: ZAB 12Mon w/c 0.50.

In Fig. 7 the cumulative pore size distribution of ZAB 12Mon w/c 0.50 are represented. The pore size distribution of neck pores was calculated using $f^*_{Gel}=f^*_{Kap}=3$ and $f^*_{Gel}=f^*_{Kap}=5$. Furthermore, the equivalent neck pores have also been computed according to 1st Method (using R_{aeq}).

Fig. 8 shows the Basis-desorption according to the three pore size distributions in Fig. 7. It can be seen that the Basis-desorption shifts toward smaller air humidities with larger form factor, since the neck pores become smaller.

All accomplished computations indicate that the second method (f^*) leads to a similar and/or better agreement with experimental results as the first method (R_{aeq}).

5.7. Worked sample: basis-desorption and primary adsorption of ZAB-2 28d w/c 0.50

The computation took place according to the IBP Method (see Sections 5.1–5.6) by considering a pore model consisting of inkbottle pores. The pore size distribution of bottle and neck pores was determined with a form factor $f^*_{cap}=3$. The saturation water content is equal to 27.8 Gew%. The pore surface ($A=88$ m2/g) and the start chemical potential ($\ln(\Delta\mu_0)=9.04$) were determined by means of the ESW-method.

The calculation of the Basis-desorption by means of the measured pore size distribution is only possible above 55% r.h.. Below this humidity the adsorption and the desorption were determined using the ESW equation. Fig. 9 shows the Basis-desorption and the primary adsorption of ZAB-2 28d w/c 0.50.

The diagram shows that the influence of inkbottle pores on drying capillary pore water is satisfactory described by a factor f^*_{cap} equal to 3.

On the other side the gel pores content (in this case 2 M.-%), which cannot be measured by means of mercury pressure porosimetry, was considered for the computation of the saturation content.

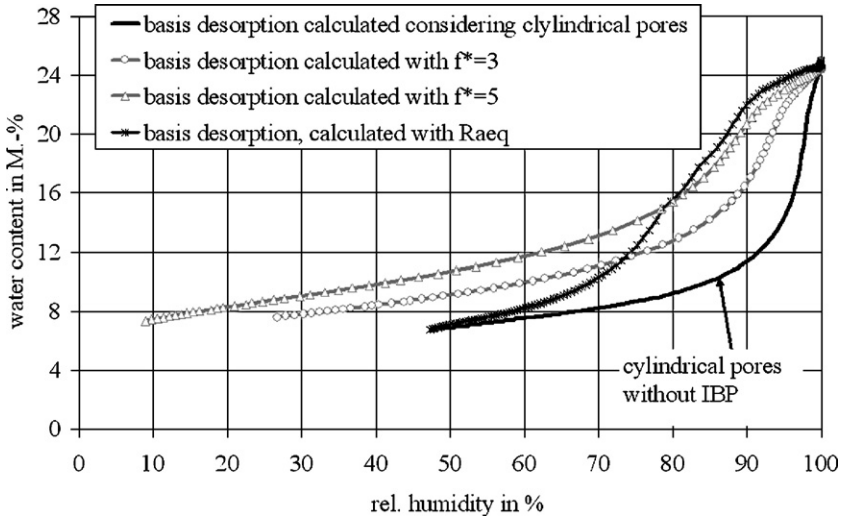

Fig. 8. Computed Basis-desorption using equivalent neck pore radii and as a function of f^*. Material: ZAB 12Mon w/c 0.50.

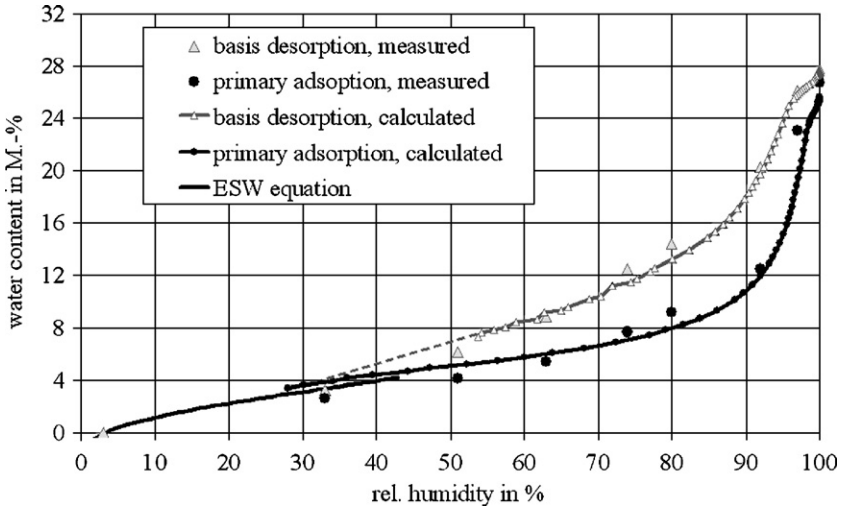

Fig. 9. Measured and by means of the IBP method computed Basis-desorption and primary adsorption of ZAB-2 28d w/c 0.50. Kind of drying: standard drying.

The formation of inkbottle pores with a neck radius smaller than 5 nm (in cement gel) could be neglected in this example. There are two reasons for this:

— The chemical aging during the Basis-desorption is still in an early stage and can therefore be neglected. After drying the chemical aging has to be considered.
— Furthermore drying to a vapour pressure smaller than 18 mbar (thus with 23 °C, $\varphi<65\%$) leads to a clear compression of cement gel. However the Basis-desorption was computed only above 60% r.h. using the pore size distribution.

The new computation method gives a satisfactory agreement with experimental results.

6. IBP method to predict scanning-isotherms

If the hygroscopic water content at changing climatic conditions is to be predicted, it is necessary to know the scanning-isotherms [11]. Since the IBP method is based on sorption thermodynamics, theoretically only hygroscopic water content can be computed.

The transition into over-hygroscopic moisture field is set at 95% r.h. Nevertheless it will be shown that the IBP method also agrees very well with measured water content within the over-hygroscopic range.

Inkbottle pores are present in the pore system according to the developed structure model [9,10]. The relation between relative humidity for capillary condensation and for capillary desorption to each pore radius $\varphi(r)$ can be deduced in meso pores by means of the Kelvin-equation (see Section 5.6.1).

As described in Section 5.6.2 in case of inkbottle pores the hysteresis between capillary condensation and capillary desorption depends on the form factor f, which gives the relation between bottle and neck pore radius:

$$f^{\mathrm{Sc}} = \frac{R_{\mathrm{F}}}{r_{\mathrm{H}}} \tag{37}$$

The larger the factor f^{Sc} is, the more pronounced the hysteresis becomes.

Furthermore it is necessary in this case to describe inkbottle pores in the gel and in the capillary pore range separately.

The following computation method can be applied to calculate scanning-isotherms. Secondary desorption, secondary adsorption, tertiary desorption etc. can be regarded as scanning-isotherms with only one branch (desorption and/or adsorption branch). Therefore they can also be computed using this method.

Required input data for the computation of scanning-isotherms are: Basis-desorption and primary adsorption as well as an assumed value for f^{Sc}.

Inkbottle pores (see Fig. 5) will be considered for the computation.

6.1. Prediction of scanning desorption isotherms

The prediction of scanning-isotherms is based on the assumption that the water content distribution depends on *material history*. Therefore the previous scanning adsorption is needed for computing the following scanning desorption. And similarly, a scanning adsorption will be computed using the previous scanning desorption. Moreover, the quantity of adsorbate w_{h} is required for correctly predicting the slope of the scanning-isotherm.

The procedure to predict scanning desorption isotherms is represented in Fig. 10. If a scanning desorption begins at the primary adsorption, it firstly follows a desorption line (d_{12}) up to the intersection with the secondary desorption at P_2. Subsequently, the desorption process lies on the secondary desorption, until a further adsorption process starts.

Each point of the primary adsorption (P_1, P_3) fulfils the following equation:

$$w_{\mathrm{ads}}(\varphi_{\mathrm{cap.cond}}) = w_{\mathrm{h}}(\varphi_{\mathrm{cap.cond}}) + w_{\mathrm{cap.cond}}(\varphi_{\mathrm{cap.cond}}) \tag{38}$$

With w_{ads} the total water content, w_{h} the quantity of adsorbate and $w_{\mathrm{cap.cond}}$ the capillary condensate amount. That total water content w^{ads} to each humidity $\varphi_{\mathrm{cap.cond}}$ is known.

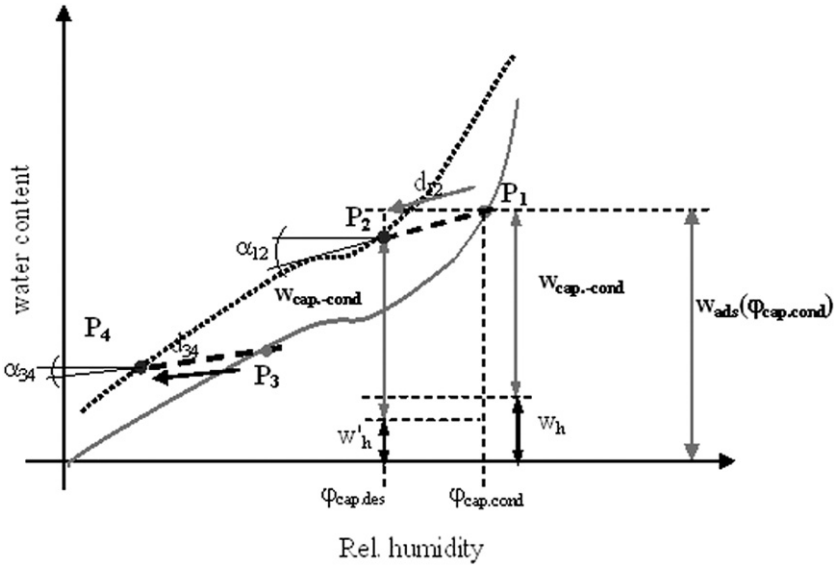

Fig. 10. Procedure to determine the scanning desorption, if the adsorption is known.

Computing the capillary condensate amount $w_{\text{cap.cond}}$ in P_1:

If the quantity of adsorbate w_h in P_1 is known, the capillary condensate amount $w_{\text{cap.cond}}$ can be computed as difference between w_{ads} and w_h:

$$w^{P_1}_{\text{cap.cond}}(\varphi_{\text{Kap.Kond}}) = w^{P_1}_{\text{ads}}(\varphi_{\text{cap.cond}})^{\text{measured}} - w^{P_1}_{h}(\varphi_{\text{cap.cond}})^{\text{calculated}} \quad (39)$$

There are several possibilities of determining the quantity of adsorbate. Once w_h can be computed with the ESW equation. Alternatively w_h can be computed considering the thickness of the adsorbate layer h:

$$w_h = h \cdot A \cdot \rho_w \cdot 100 \text{ in } M.-\% \quad (40)$$

With A the specific pore surface and ρ_w the density of the water.

The smaller the pores are, the more distinctive the influence of h becomes. Therefore it may not be neglected and it will be calculated according to:

$$h(\varphi) = 0.395 - 0.189 \cdot \ln(-\ln(\varphi)) \text{ in nm} \quad (41)$$

Computing a desorption line d_{12}

The scanning desorption begins at P_1. Due to hysteresis the capillary desorption cannot take place immediately at $\varphi_{\text{cap.cond}}$, but at a smaller humidity $\varphi_{\text{cap.des}}$. Hence the capillary condensate volume $w^{P1}{}_{\text{cap.cond}}$ remains constant during desorption (d_{12}) until $\varphi_{\text{cap.des}}$ is reached. Only the quantity of adsorbate must decrease according to Eq. (41), since the relative humidity decreases.

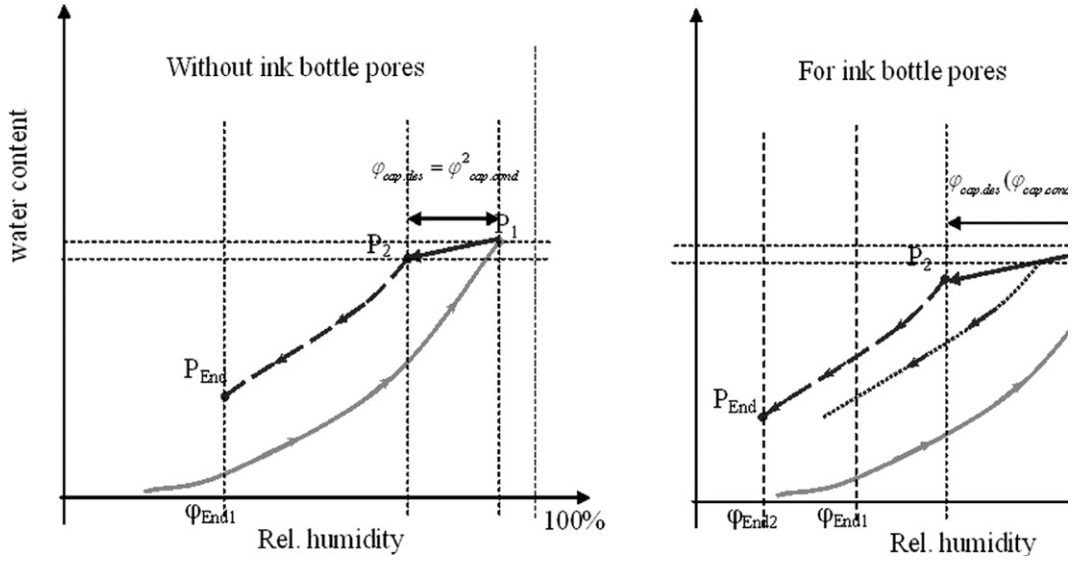

Fig. 11. Calculation of relative humidity for capillary desorption $\varphi_{\text{cap.des}}$ in case of known $\varphi_{\text{cap.cond}}$.

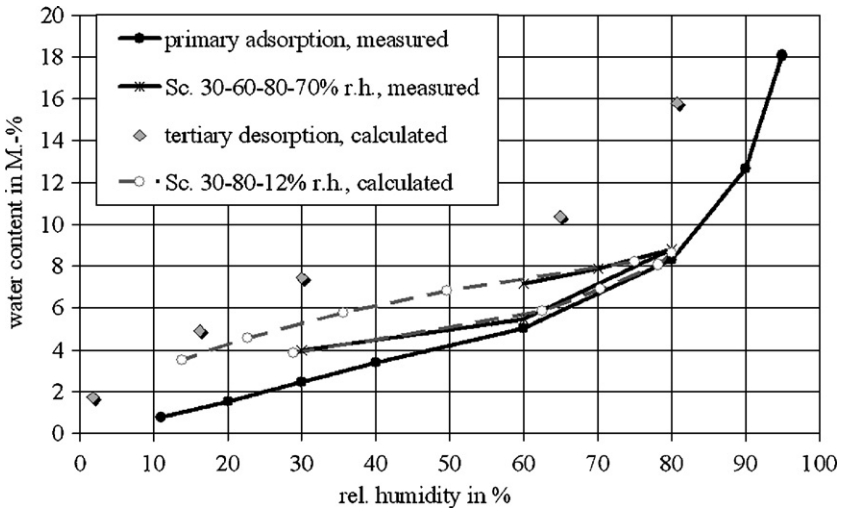

Fig. 12. Measured and computed Scanning-isotherm 30–60–80–30% r.h. Material: ZAB 12Mon w/c 0.60. Kind of drying: standard drying.

Each point on the desorption line (d_{12}) including P_2 fulfil:

$$w_{\mathrm{des}}^{d_{12}}(\varphi_{\mathrm{cap.des}} \leq \varphi < \varphi_{\mathrm{cap.cond}}) = w_{\mathrm{h}}^{\mathrm{d12}}(\varphi) + w_{\mathrm{cap.cond}}^{\mathrm{P_1}}(\varphi_{\mathrm{cap.cond}}) \tag{42}$$

A desorption line (as d_{12}, d_{34}) can be computed from each point on the adsorption isotherm. The connection of the end points of each desorption line (P_2, P_4) gives the desorption isotherm (e.g. the secondary desorption). In the following, the calculation of the end point of each desorption line will be explained.

Calculation of the relative humidity for capillary desorption $\varphi_{\mathrm{cap.des}}$ (P_2)

For cylindrical pores it follows approximately:

$$\varphi_{\mathrm{cap.des}} \approx \varphi_{\mathrm{cap.cond}}^2 \tag{43}$$

For modelling inkbottle pores the following equation is used:

$$\ln\varphi_{\mathrm{cap.des}} = \frac{f^{\mathrm{Sc}} \cdot r_{\mathrm{H}} - h(\varphi_{\mathrm{cap.cond}})}{r_{\mathrm{H}} - h(\varphi_{\mathrm{cap.des}})} \cdot \ln\varphi_{\mathrm{cap.cond}} \tag{44}$$

The resulting hysteresis is represented schematically in the Fig. 11.

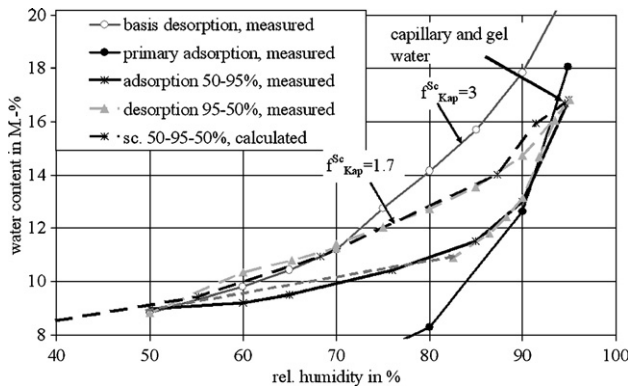

Fig. 13. Measured and computed Scanning-isotherm 50–95–50% r.h.. Material: ZAB 12Mon w/c 0.60. Drying method: standard drying.

The computation of the relative humidity for the capillary desorption and the appropriate water content $w_{\mathrm{h}}(\varphi)$ requires an iterative solution procedure using Eqs. (39) and (44).

6.2. Prediction of scanning adsorption isotherms

Consider a scanning adsorption, which begins at a known primary desorption (e.g. the secondary desorption). At first it follows an adsorption line (a_{12}) up to the intersection with the secondary adsorption. Afterwards, the adsorption process lies on the secondary adsorption, until a further desorption process starts. Thus it is possible to predict the secondary adsorption by joining each end-point of the adsorption lines.

Each point of the known desorption fulfils the following equation:

$$w_{\mathrm{des}}(\varphi_{\mathrm{cap.des}}) = w_{\mathrm{h}}(\varphi_{\mathrm{cap.des}}) + w_{\mathrm{cap.cond}}(\varphi_{\mathrm{cap.des}}) \tag{45}$$

As shown in Section 6.1 the capillary condensate content $w_{\mathrm{cap.cond}}$ in Eq. (46) can be computed. This remains constant during the adsorption between $\varphi_{\mathrm{cap.des}}$ and the computed humidity $\varphi_{\mathrm{cap.cond}}$, which depends on f^{Sc}.

Thus the adsorption line a_{12} results:

$$w_{\mathrm{ads}}^{\mathrm{a12}}(\varphi_{\mathrm{cap.des}} < \varphi \leq \varphi_{\mathrm{cap.cond}}) = w_{\mathrm{h}}^{\mathrm{a12}}(\varphi) + w_{\mathrm{cap.cond}}(\varphi_{\mathrm{cap.des}}) \tag{46}$$

The quantity of adsorbate w_{h} will be computed with Eq. (40). The solution of the system of equations consisting of Eqs. (40) and (45) is iterative.

6.3. Slope of scanning-isotherms

The components of water content are represented in Fig. 10. The capillary condensate remains constant between P_1 and P_2 but not the adsorbed water w_{h}. Hence it follows that the

branch of the scanning-isotherm (d_{12} or a_{12}) exhibits a slope α_{12} given by:

$$\alpha_{ij} = \frac{w_h(\varphi_{cap.cond,i}) - w_h(\varphi^2_{cap.cond,j})}{\varphi_{cap.cond,i} - \varphi^2_{cap.cond,j}}$$

$$\text{and for ink bottle pores } \alpha_{ij} = \frac{w_h(\varphi_{cap.cond,i}) - w_h(\varphi_{cap.des,j})}{\varphi_{cap.cond,i} - \varphi_{cap.des,j}} \quad (47)$$

It must be noted that the slope depends on the relative humidity and on the form factor. Thus the slope of the scanning-isotherms can be estimated in advance. This is very interesting for the numerical simulation of heat and water transport, since the slope can be regarded as a material parameter for the determination of the scanning-isotherms.

6.4. Worked sample

6.4.1. Scanning-isotherm 30–60–80–70% r.h.

Fig. 12 shows the calculated and the measured scanning-isotherm 30–60–80–70% r.h. [8]. A good agreement with the experimental results is given.

6.4.2. Scanning-isotherm 50–95–50% r.h.

For this example a water-saturated hardened cement paste at the age of 15 month with w/c 0.60 was used (Fig. 13).

Using the known Basis-desorption, the adsorption branch 50% to 95% r.h. was computed. The effect of inkbottle pores within the range of capillary porosity was considered with a factor $f^{Sc}_{cap}=3$. The chemical aging of cement gel can be neglected, since the material was only dried at 50% r.L.

The following desorption begins at a saturation rate equal to 62%. Therefore the influence of inkbottle pores for the computation of the second desorption has to be considered by a smaller factor f^{Sc}_{cap}. A for factor $f^{Sc}_{cap}=1.7$ leads to a very good agreement with the experimental results.

7. Conclusions

Owing to the complex geometrical characteristics of a random microstructure in cementitious materials, it has to be expected that pores shapes like inkbottles exists. In [10] it was shown that inkbottle pores with very small necks (< 1 nm) form during the freezing-drying process. The reason for it is that very strong binding forces between micro pore water and material has to be broken in order to dry micro pore water and a compression of the CSH-phases takes place. Hence it remains a great amount of water up to very low relative humidities.

Cement hydration and chemical aging also influence sorption isotherms and hysteresis according to own results in Refs. [9] and [10].

The IBP-method calculates Basis-desorption and primary adsorption using the saturation water content, the pore size distribution and two form factors for the inkbottle pores (for the capillary and gel porosity).

For the computation of the scanning-isotherms it is necessary to know whether a previous desorption or a previous adsorption isotherm. The history of the water content in the pore size distribution is required to predict the water content in following adsorption and desorption procedures. The two form factors for the inkbottle pores (for the capillary and gel porosity) are also necessary.

The developed IBP method allows a reliable prediction of the hygroscopic and over-hygroscopic water content in hardened cement paste in equilibrium at changing climatic conditions. More calculated scanning-isotherms can be found in Ref. [9]. So far the procedure is only verified for Portland cement. An application of the developed procedure on other cements is possible in principle, since the procedure was deduced theoretically. A few short-time experiments as well as the analysis of the pore structure by means of mercury pressure porosimetry are necessary for the adjustment of the form factor to pore structure.

References

[1] J. Adolphs, M.J. Setzer, A Model to Describe Sorption Isotherms, Journal of Colloid and Interface Science 180 (1996) 70–76.

[2] J. Adolphs, M.J. Setzer, ESW- Eine neue Methode zur Auswertung von Sorptionsisothermen, GDCh-Monographie Band 7, Bauchemie, 1. workshop, S.33 ff(1997).

[3] J. Adolphs, Thermodynamische Beschreibung der Sorption, Diss.1994, Universität GH Essen.

[4] Z.P. Bazant, Thermodynamics of hintered sorption and its implications for hardened cement paste and concrete, Cement and Concrete Research 2 (1) (1972) 1–16 (S.).

[5] J.C.P. Broekhoff, Adsorption and Capillarity, Thesis at Delft University of Technology, Delft, Waltman, 1969.

[6] N.V. Chuarev, G. Starke, J. Adolphs, Isotherms of Capillary Condensation Influenced by Formation of A Sorption Film: 1. Calculation for Model Cylindrical and Slit Pores, Journal of Colloid and Interface Science 221 (2000) 246–253.

[7] B.V. Derjaguin, Theory of Stability of Colloids and Thin Films, Plenum Press, New York, 1989.

[8] R.M. Espinosa, L. Franke, Sorptionsisotherme für Zementstein, 5, Int. Kolloqium Werkstoffwissenschaften und Bauinstandsetzen, Esslingen 1999, Symp, Bericht Aedificatio Publishers, Freiburg, 1999, Band II.

[9] R.M. Espinosa, Sorptionsisothermen von Zementstein und Mörtel, Dissertation Technische Universität Hamburg–Harburg, 2004.

[10] R.M. Espinosa, L. Franke, Influence of the age and drying process on pore structure and sorption isotherms of hardened cement paste, Cement and Concrete Research 36 (2006) 1971–1986.

[11] R.F. Feldman, Sorption and length-change scanning-isotherms of methanol and water on hydrated Portland cement, Proceedings of the 5th International Congress on the Chemistry of Cement, vol. 3, Cement Association of Japan, Tokyo, 1968, pp. 53–68, S.

[12] J.W. Gibbs, The Scientific Papers of J. Willard Gibbs, Thermodynamics, vol. 1, 1993.

[13] S.J. Gregg, K.S.W. Sing, Sorption, Surface Area and Porosity, Academic Press, London, 1982.

[14] J. Grunewald, Diffusiver und konvektiver Stoff-und Energietransport in kapillarporösen Baustoffen, Dissertation, Univ. Dresden 1997.

[15] K.K. Hansen, Sorption Isotherms, A Catalogue, 1986.

[16] H.M. Künzel, Verfahren zur ein-und zweidimensionalen Berechnung des gekoppelten Wärme-und Feuchtetransports in Bauteilen mit einfachen Kennwerten. Diss. Univ. Stuttgart 1994.

[17] T.C. Powers, Properties of Cement Paste and Concrete. Paper V-1. Physical properties of Cement Paste, Proceedings of the Fourth International Symposium on the Chemistry of Cement, 1960.

[18] M.J. Setzer, P. Heine, J. Adolphs, Mercury pressure porosimetry, Kontaktwinkel und andere Eigenschaften von Zementstein bei verschiedenen Luftfeuchten, Fachtagung Quecksilberporosimetrie an Baustoffen, BAM Berlin 2/2000.
[19] M.J. Setzer, Oberflächenenergie und mechanische Eigenschaften des Zementsteins, Dissertation 1972, Technische Universität München.
[20] H. Splittgerber, F. Wittmann, Sorptionsmessungen an erhärtetem Zementstein, Zement-Kalk-Gips 10 (1996) 493–496.
[21] J. Stark, B. Möser, A. Eckart, Neue Ansätze zur Zementhydratation, ZKG international Nr. 1/2001 (Teil 1) und Nr. 2/2001 (Teil 2).
[22] J. Thomas, H. Jennings, Chemical Aging and the colloidal Structure of the CSH-Gel: Implications for creep and shrinkage. Implications for creep and shrinkage, in Creep, Shrinkage and Durability Mechanics of Concrete and Other Quasi-Brittle Materials: Proceedings of the Sixth International Conference, Concreep-US-Ulm, F. J., Bazant, Zdenek P., Wittmann, Folker H. 2001/08 Pergamon Pr.
[23] J. Thomas, H. Jennings, A. Allen, The surface area of hardened cement paste as measured by various techniques, Concrete Science and Engineering 1 (1999) 45–64.
[24] J. Thomas, H. Jennings, A colloidal Interpretation of chemical aging of the CSH gel and its effects on the properties of cement past, Cement and Concrete Research 36 (1) (2006) 30–38.
[25] D.N Winslow, M.D. Cohen, D.P. Bentz, K.A. Snyder, E.J. Garboczi, Percolation and pore structure in mortars and concrete, Cement and Concrete Research 24 (1994) 25–37.
[26] F.H. Wittmann, Interaction of hardened Cement Paste and Water, Journal of American Ceramics Society 56 (8) (1973) 409–415.